Direct comparison of a 1 V Josephson arbitrary waveform synthesizer and an ac quantum voltmeter

2015 Metrologia 52 528

(http://iopscience.iop.org/0026-1394/52/4/528)

IOP Publishing | Bureau International des Poids et Mesures Metrologia

Metrologia **52** (2015) 528–537 doi:10.1088/0026-1394/52/4/528

Direct comparison of a 1 V Josephson arbitrary waveform synthesizer and an ac quantum voltmeter

Ralf Behr, Oliver Kieler, Jinni Lee, Stephan Bauer, Luis Palafox and Johannes Kohlmann

Physikalisch-Technische Bundesanstalt, Braunschweig, Germany

E-mail: ralf.behr@ptb.de

Received 10 April 2015, revised 22 May 2015
Accepted for publication 26 May 2015
Published 16 June 2015

Abstract

AC Josephson voltage standards based on pulse-driven Josephson arrays (Josephson arbitrary waveform synthesizer—JAWS) have recently achieved an output voltage of at least 1 V root-mean-square. An ac quantum voltmeter (ac-QVM) based on a 2 V programmable Josephson array has been used to verify the quantization level of the new JAWS by performing a direct comparison in the frequency range from 30 Hz to 2 kHz. The comparison has demonstrated an excellent agreement between the two quantum standards of better than 1 part in 10^8. Sources for systematic errors have been investigated. The overall uncertainty is found to be better than 1.2 parts in 10^8 ($k = 1$) for measurements at a frequency of 250 Hz and 1 V amplitude.

Keywords: ac Josephson voltage standard, Josephson arbitrary waveform synthesizer, ac quantum voltmeter, direct comparison

(Some figures may appear in colour only in the online journal)

1. Introduction

Many years after the first realization of a pulse-driven ac Josephson voltage standard in 1996 [1], recent developments in Josephson Arbitrary Waveform Synthesizer (JAWS) led to the major breakthrough of achieving 1 V RMS output voltages [2–4]. The JAWS is already used in several National Metrology Institutes (NMI) in special applications where only 100 mV levels are required e.g. for ac–dc transfer measurements [5–9] and for calibrating ac voltage standards and instruments [10–12]. The increase to the 1 V level is important for many metrological applications, as instruments and measurement methods are consequently more accurate in that range [13–16].

For the JAWS, the Josephson junctions are operated by short current pulses which effect a transfer of flux quanta across the barriers. According to the Josephson equation, a time-dependent voltage, which is quantized at all times, is generated at the output leads of the junction series array:

$$V(t) = n \cdot m \cdot \Phi_0 \cdot f_p(t) \quad (1)$$

The time dependent output voltage $V(t)$ is the product of the Shapiro-step number n, the number of junctions in the series array m, the flux quantum $\Phi_0 = h/2e$ (h is Planck's constant and e the elementary charge), and the repetition frequency of the pulses $f_p(t)$. Typical maximum pulse-repetition frequencies used for the JAWS are 15 GHz, limited by the maximum clock frequencies ($f_{clock-PPG}$) of commercially available pulse pattern generators (PPG). In practice, this maximum time dependent voltage is reduced by a $\Sigma\Delta$ amplitude factor, $A_{\Sigma\Delta} < 1$ in order to achieve the desired spectral purity of the waveforms.

A big advantage of the JAWS is that signals can be synthesized over a very wide frequency range from a few hertz up to a few megahertz [17] and dc voltages. In theory, this approach for the synthesis of quantized ac waveforms enables the generation of voltage signals of excellent spectral purity with low noise and no drift. However, as is the case for dc Josephson

systems, the output voltage has to be verified by investigations and comparisons. A direct on-chip comparison of two JAWS sine waves has been performed at small amplitudes of about 10 mV with a relative uncertainty of 3×10^{-8} [18], but both voltages agreed within 2×10^{-8} only without the compensation signals commonly used in the ac coupling technique [19]. Indirect comparisons between a JAWS and a programmable Josephson voltage standard (PJVS) have been performed via a ΣΔ-ADC as transfer instrument [20–22]. At the 100 mV level and 500 Hz Jeanneret *et al* [21] achieved a very good agreement of 2×10^{-7}.

This paper describes a direct verification of the new 1 V RMS JAWS system at PTB after recent improvements. For the verification of operating margins, another quantum based voltage standard—the ac quantum voltmeter (ac-QVM)—has been used. The ac-QVM, introduced in 2006 [23], had in the past been successfully employed for sine waves [24–26] and recently to calibrate commercial calibrators up to 7 V RMS and frequencies into the kHz range [27–29]. In this paper, the system has been used to verify the waveforms generated by the JAWS in the frequency range 30 Hz to 2 kHz.

2. Systems and setups

2.1. The JAWS

This section is a brief summary of the JAWS system at PTB and its recent improvements. A detailed description of the system is given in [4]. The combination of improvements pursued at PTB (e.g. optimized shielding of cables used for the compensation signal and grounding of the experimental setup) resulted in better operating margins and less crosstalk at the target voltage of 1 V RMS. We use 21 000 triple-stacked Josephson junctions in eight arrays to achieve the 1 V level. Both positive and negative pulses are generated by a commercially available PPG (Sympuls BPG 30-TER[1]) with a clock rate of 15 GHz. We use the ac coupling method introduced by Benz *et al* [18] with four dual arbitrary waveform generators for the compensation signals (Agilent 33522B[1]). One of them acts as master for the synchronization of the whole system, both the JAWS on its own and also for the ac quantum voltmeter. All compensation signals are isolated by PTB built electronics. To achieve the 1 V RMS output voltage with 63 000 junctions at a clock frequency of 15 GHz, we calculated a sigma-delta code with a code-amplitude of about 72.37%. Figure 1 shows the frequency spectrum of a synthesized 1 V RMS sine wave. Higher harmonics are suppressed down to −121 dBc, whereas the noise floor is as low as −140 dBc. Compared to [4] the improvements in the setup have resulted in a significant reduction of the unwanted harmonics.

2.2. The ac quantum voltmeter

Quantum based differential sampling was introduced in 2006 [23] and has since then been further investigated towards higher voltages and frequencies [24–31]. A waveform constructed with quantized steps is synchronized to the waveform under test, and their difference is measured. The waveform

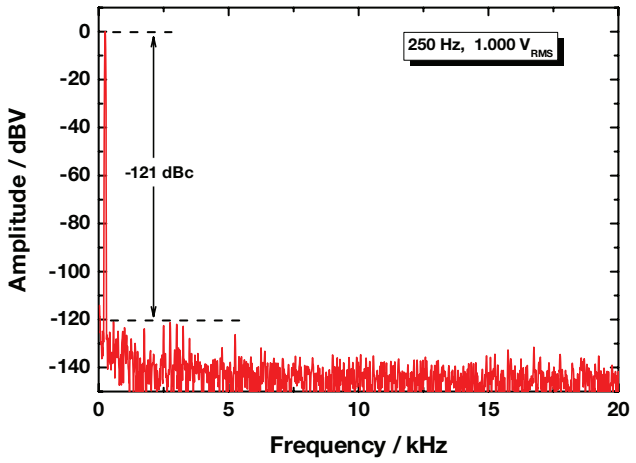

Figure 1. Frequency spectrum of a synthesized sinusoidal waveform generated by 8 arrays in series ($f = 250$ Hz, $V_{RMS} = 1$ V, $m = 63\,000$, $f_{clock-PPG} = 15$ GHz, $A_{\Sigma\Delta} = 0.7$, 1 MΩ input impedance and 10 V_{p-p}-range of the PXI).

under test is reconstructed from measured differences and their associated Josephson voltage steps. The RMS value of this reconstructed waveform is then calculated. The frequency spectrum can also be determined. As described in [28], the number of samples is a compromise between the frequency being measured, the maximum permissible voltage difference at the input of the null detector, and the settling time, including the null detector, around each transition between quantized voltage levels.

The ac-QVM uses a commercially available NPL bias source[1] [32] to drive a programmable 2 V array with 16384 (8192 double-stacked) Josephson junctions with a critical current of 3.2 mA and operating at 70 GHz [33]. The system is electrically isolated and the computer is connected via an optical ring [34]. Each of the 14 segments in the binary divided Josephson array is driven by a separate channel of the bias source. The channels have an amplitude resolution of 14 bit and the transitions at the output of the array have rise times below 200 ns without using a method suppressing reflections [35].

The system uses a programmable 70 GHz microwave synthesizer [36]. The microwave power is set to 50 mW for equal step widths for the zero and first voltage steps. The margins are 2.05 mA wide, which means that after setting the array bias currents, we usually can run the system for weeks without re-adjusting the parameter settings. In particular, no parameter changes are required within the duration of the measurements presented in this paper.

The ac quantum voltmeter uses a battery powered ΣΔ-analogue-to-digital converter (ΣΔ-ADC) as sampler. Hence the whole ac-QVM is electrically isolated. The setup for the direct comparison is schematically shown in figure 2. For simplicity the JAWS is presented by just one array. On-chip low-pass filters are labeled with 'F' [37]. The trigger and clock signals, which are optically isolated, are generated by the JAWS to synchronize the ΣΔ-ADC and the PJVS bias

[1] Identification of commercial equipment does not imply an endorsement by PTB or that it is the best available for the purpose.

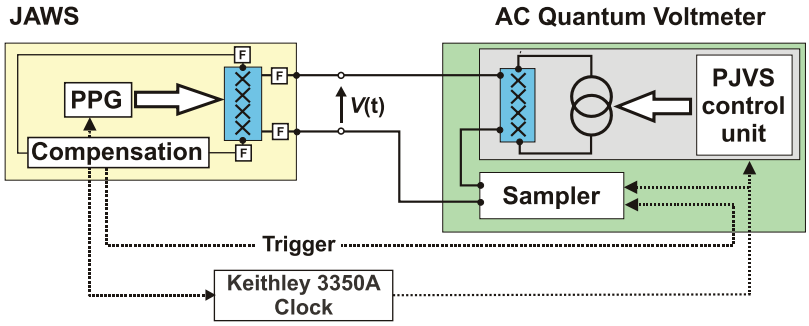

Figure 2. Measurement setup for the direct comparison between the JAWS and the ac Quantum Voltmeter. Dotted lines show the synchronization signals.

source. A waveform generator (Keithley 3350A[1]) is used to set the phase shift between the JAWS waveform and the ac-QVM stepwise approximated sine wave. The precise phase adjustment is done manually by de-tuning the 20 MHz clock until the RMS value of the difference at the ΣΔ-ADC indicates the lowest signal amplitude. This lowest signal amplitude is reached for smallest voltage differences at the ΣΔ-ADC which are achieved when the sine wave crosses precisely the centers of the PJVS steps [28]. The maximum frequency for the method is limited by the speed of the sampling detector and the number of points that have to be discarded around each transition between quantized voltage steps [21–31]. We selected the NI PXI 5922A card[1] for our measurements and operated it in the $2\,V_{p-p}$ range at $4\,MS\,s^{-1}$ and $10\,MS\,s^{-1}$ sample rates.

3. JAWS operating margins

In this section we briefly describe the JAWS parameter settings and the determination of the operating margins. For each channel we have to adjust four operating parameters: positive and negative pulse-amplitude, compensation signal amplitude and the phase. We normally start with the adjustment of the positive and negative pulse amplitudes for a sinusoidal waveform with small output voltage amplitude (e.g. about 10 mV), where no compensation is necessary. A sweep current is applied to the array to evaluate the Shapiro step under pulses. The maximum sweep current, where the frequency spectrum of the synthesized waveform remains unchanged (i.e. pure spectrum with no higher harmonics), is called the current margin of the array. Then we increase the sinusoidal output voltage by increasing the ΣΔ-code-amplitude, and the compensation amplitude and phase are adjusted to ensure maximum current margins. This method is repeated for each array. After the adjustment of each array, all 8 arrays are switched on and a final minor adjustment is performed to compensate for any crosstalk between the electrical signals (mainly compensation signal crosstalk). When all arrays are in operation, the overall current margins are also determined—i.e. the common Shapiro step widths under pulses for all junctions.

For the 250 Hz signal in figure 1 we established a current margin of 160 μA, which is limited by the 'weakest' array. The current margins become smaller for higher frequencies, e.g. about 70 μA for 2 kHz. However, these values are still more than sufficient for stable operation of the JAWS during the comparison described in this paper. The other seven arrays show current margins between 500 μA and 1.1 mA at 250 Hz.

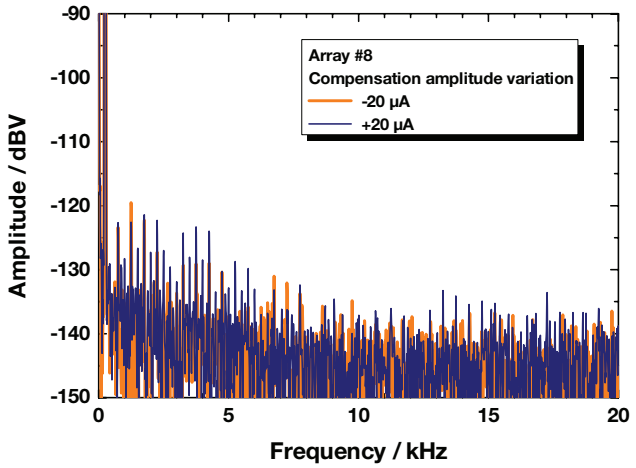

Figure 3. Two frequency spectra of a synthesized sinusoidal waveform generated by array #8 ($f = 250$ Hz, $V_{RMS} = 0.143$ V, $m = 9000$, $f_{clock-PPG} = 15$ GHz, $A_{\Sigma\Delta} = 0.7$, 1 MΩ input impedance and $10\,V_{p-p}$-range of the PXI). The compensation amplitude is varied from −20 μA to +20 μA relative to optimum setting.

The JAWS experimental setup is fully computer controlled and all 32 operating parameters for the 8 arrays are stored in a computer program and can be reapplied by pressing a button. These operating parameters are stable in time even after recooling on a number of occasions. Small electrical drifts of the parameters of the PPG and the compensation electronics are fully compensated by the broad and stable operating margins of the JAWS arrays, i.e. no readjustment was necessary over a period of six months.

The phase for the compensation current is set with a resolution of 0.1 degrees within a typical range (arrays #1 − 7) to be 'on margins' of more than 300 μA at 250 Hz. Figure 3 shows directly measured two zoomed-in spectra of array #8 at 250 Hz. The difference between the two spectra is the parameter setting for the compensation current ±20 μA, respectively. Only small variations of some higher harmonics are visible due to this parameter variation. From these variations it is difficult to decide about 'margins' especially when having in mind that the spectrum is affected by nonlinearities of the ΣΔ-ADC and crosstalk between channels. In this way we measured the RMS value of the fundamental tone for all arrays.

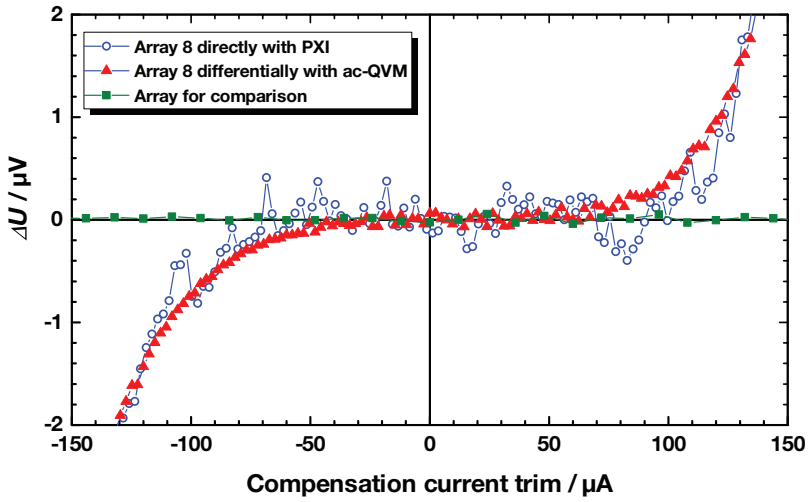

Figure 4. Change in RMS voltage of the fundamental for two different arrays as a function of compensation current. The margins for array #8 (smallest margins) have been measured directly with the ΣΔ-ADC (blue circles) and using the ac-QVM (red triangles).

In figure 4 the variation of the output voltage, ΔU, relative to optimum setting at 0 μA is plotted as a function of the compensation current trim for two different arrays. All other settings are the same as for figure 3. The 'margins' depend on the uncertainty of the measurement method which refers here to 0.4 μV for the direct measurement and 0.05 μV for the differential method with the ac-QVM. Arrays #1 to #7 have typical margins and show constant voltage for variations of the compensation current over ± 150 μA, as depicted by the green squares (measured with the differential sampling technique). Only array #8, the 'weakest one', has considerably smaller margins than the other seven arrays. Array #8 has been measured 1) directly, using the ΣΔ-ADC (blue circles) and 2) with the ac-QVM using the differential sampling technique [38] (red triangles). The measurement time for one compensation current sweep has been set to 20 min which makes a good balance between achievable resolution and drift of the ΣΔ-ADC. The direct measurement suggests flat margins for compensation currents from −70 μA to +90 μA. However, when measured with a higher resolution system (the ac-QVM), the margins for the compensation current become evidently smaller and in fact span only from −30 μA to +40 μA. We also evaluated the stability of the compensation current and found that it varied by $\leqslant$1 μA in ten minutes. This small variation of compensation current does not influence our measurements. As is the case when looking at dc voltages from Josephson arrays, higher resolution for the voltage measurement, in this case from the ac-QVM, results in a reduction of the experimentally determined step width. Here we have connected two Josephson system and we cannot completely rule out that part of the reduction is due to a small electromagnetic interference (EMI) between the two systems.

4. Comparison measurements and results

4.1. Settings for differential sampling

It is important to be aware of the high speed sampler's response to the transients in programmable stepwise waveforms in the ac-QVM [39, 40]. The readings of the ΣΔ-ADC show the same ringing structure before and after the voltage of the array changes. The ΣΔ-ADC step response has been investigated for the ac-QVM in former papers [28, 29]. As in our previous investigations, the '48-tap standard' finite-impulse-response filter has been used as this filter has the flattest frequency response out of the four available [41]. The calculation of the RMS value (for the reconstructed waveform at the input of the ΣΔ-ADC) needs to remove a fixed number of readings before and after the transients. This procedure has been published earlier [28, 29, 42]. The number of points that need to be removed is independent of the sampling frequency used. As our aim was to achieve the best uncertainties possible, even below the μV V^{-1} level in previous works, we always investigated carefully the impact on the RMS voltage of the number of readings deleted around the transients. Additionally, the quantum nature of the JAWS waveforms, with lower noise, no drift and higher stability, was expected to confirm that the μV V^{-1} uncertainty established previously was a result of the waveform generator. In order to use as many points as possible and to reduce the limitation towards frequencies above 1 kHz, we usually deleted 30 points before and 30 points after each step transition. A very similar analysis has been performed in a measurement setup where the ΣΔ-ADC was used as a transfer standard [40, 42].

The parameters that need to be established are: 1) the phase between the signal to be measured and the stepwise approximated waveform in the ac-QVM, 2) the number of steps per period in the Josephson waveform, and 3) the ΣΔ-ADC sample rate. For most frequencies a sample rate of 4 MS s^{-1} has been chosen. In order to verify the results, some frequencies have been measured using a sample rate of 10 MS s^{-1}. As reported in [28], changing the sampling rate has a clear effect on the gain of the ΣΔ-ADC. In order to avoid these changes, we performed the measurements in groups with constant sample rates. The sine waves have been approximated with 20 Josephson steps per period. Fine tuning of the phase is not required, as shown by Lee *et al* [28].

We used a JAWS-off and JAWS-on procedure for all frequencies to calibrate the gain, G, and offset of the ΣΔ-ADC

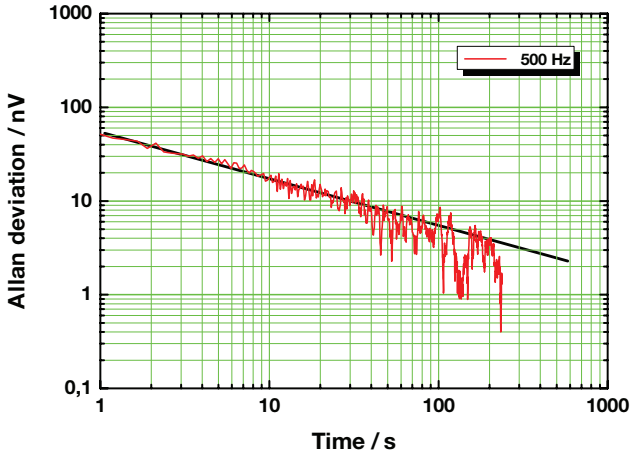

Figure 5. Typical Allan deviation analysis for $f = 500\,\text{Hz}$ and $V_{\text{RMS}} = 1\,\text{V}$ using the $2\,\text{V}_{\text{p–p}}$-range and $4\,\text{MS}\,\text{s}^{-1}$ sample rate of the ΣΔ-ADC in the ac-QVM.

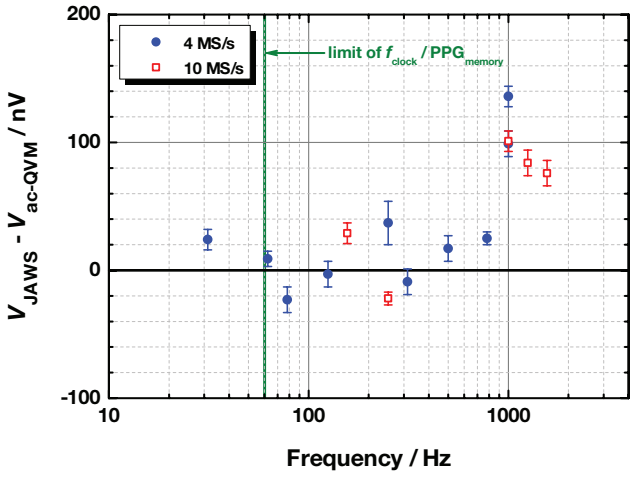

Figure 6. Frequency dependence of measured deviation of JAWS from theoretical value at $1\,\text{V}_{\text{RMS}}$. The error bars are type-A uncertainties ($k = 1$).

without the need for any switches in the measurement setup. First we turn off the JAWS thus realizing a superconducting short circuit. The PJVS peak amplitude was set to 150 mV, the expected amplitude at the ΣΔ-ADC in the differential measurement. The offset and gain of the ΣΔ-ADC are determined within one minute using the Josephson waveform synthesizer of the ac-QVM to generate a stepwise approximated waveform. That waveform is measured by the ΣΔ-ADC and a linear fit to the voltage steps is made [28, 43]. Then, we turn on the JAWS, set the PJVS peak amplitude to 1.414 V, synchronize the two systems and measure the JAWS RMS amplitude with the ac-QVM. Each measurement point is adjusted by its corresponding gain and offset values.

4.2. Allan deviation analysis

Before starting a long set of measurements it is always useful to perform an Allan analysis [44]. Such an analysis provides information about the uncertainty that can be achieved and helps optimizing the duration of the experiment. For differential measurements the uncertainty limit varies slightly with frequency, amplitude being measured, and sampling rate of the ΣΔ-ADC in the $2\,\text{V}_{\text{p–p}}$-range. Consequently the Allan deviation has been analysed for all measurements of the JAWS RMS voltage. A typical set is shown in figure 5. All data are in the white noise regime after one second and up to at least 100 s. The corresponding uncertainty ($k = 1$) after one-minute measurement time is typically below 10 nV (1×10^{-8}). This noise level is significantly lower compared to previous papers, where the limit was determined by the noise, drift or jitter of the synthesizer being measured [28, 29, 39]. When the ac-QVM measures a JAWS waveform, the setup is limited by the ΣΔ-ADC alone, as proven by the similarity with a shorted ΣΔ-ADC. As expected, both Josephson systems do not contribute additional noise. Based on this analysis, we collect readings for about 100 s and the type-A uncertainty is given by the Allan deviation analysis.

4.3. Comparison results

Results of the direct comparison are shown in figure 6 for the frequency range from 30 Hz to 1.5 kHz at an amplitude of 1 V RMS. The error bars indicate the type-A uncertainty ($k = 1$) given by the Allan analysis. Measurements were taken with two different sampling rates, namely $4\,\text{MS}\,\text{s}^{-1}$ and $10\,\text{MS}\,\text{s}^{-1}$. For frequencies below 1 kHz, all measured RMS voltages of the JAWS agree within 4×10^{-8} with the theoretical value of the JAWS (equation (1)). A deviation of about 1×10^{-7} is visible for frequencies between 1 kHz and 1.5 kHz. Above 1.5 kHz, the deviation increases rapidly and reaches about $6\,\mu\text{V}\,\text{V}^{-1}$ at 2 kHz. This increase is steeper than e.g. a ω^2-behaviour and needs further investigation.

Remarkably, the lowest frequency, 30 Hz, shows good agreement with the theoretical result. This constitutes an extraordinary result as this frequency cannot be synthesized in the usual way. Normally, the lowest frequency in a JAWS is given by the clock frequency divided by the PPG memory e.g. $f_{\text{clock–PPG}} = 15\,\text{GHz} / 256\,\text{MBit} \approx 58\,\text{Hz}$. Our PPG can be programmed to repeat each pulse up to 32 times before going to the next position in the pattern [45]. This first test shows excellent results for a pattern calculated for 60 Hz and each pulse repeated twice. Additional tests may require special codes to take account of the repeated pulses. This feature will allow a further reduction in synthesized frequencies down to 1.8 Hz without reducing the clock frequency or increasing the physical memory of the PPG.

For an intermediate frequency of 250 Hz we decided to take a larger series of measurements, as shown in figure 7. All data taken on three different days are summarized. The difference between the mean of all 14 measurements and the theoretical value of the JAWS (equation (1)) is +3.5 nV ($3.5 \times 10^{-9}\,\text{V}\,\text{V}^{-1}$) as indicated by the blue solid line in the figure. The standard deviation of the mean for these fourteen measurements is 5.0 nV ($k = 1$) and indicated by the dashed lines. The combined uncertainty is calculated in the following section.

5. Discussion and uncertainty investigations

We performed a number of investigations in order to validate the performance of the JAWS thoroughly. The uncertainty

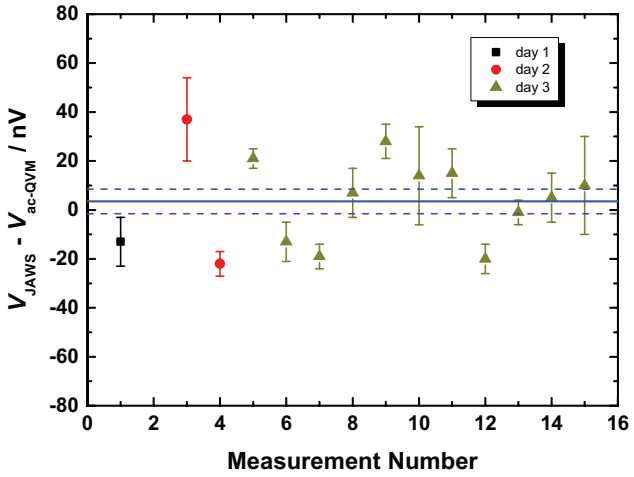

Figure 7. Individual measurement points of the JAWS and the ac-QVM for a 1 V sine wave of 250 Hz measured on three different days. The error bars show the type-A uncertainties ($k = 1$). The solid line represents the mean value at +3.5 nV and the experimental standard deviation of the mean of the 14 individual measurement points ($k = 1$) is represented by the dashed lines.

Table 1. Uncertainty budget for the comparison at 250 Hz ($k = 1$).

Component	Estimate ($\mathrm{nV\,V^{-1}}$)	Distribution	Uncertainty ($\mathrm{nV\,V^{-1}}$)
Type-A			
Measurement (14 data points)	5.02	Normal	5.02
Type-B			
MW Frequency	0.004	Normal	0.004
ΣΔ-ADC gain	15.0	Rectangular	8.7
ΣΔ-ADC INL	5.0	Rectangular	2.9
ΣΔ-ADC bandwidth	5.0	Rectangular	2.9
Cable correction	0.43	Normal	0.43
On-chip inductance, phase error	3.1	Normal	3.1
Sloped step	7.2	Rectangular	4.2
Total			**11.7**

budget for the comparison between JAWS and ac-QVM was also evaluated. This uncertainty budget is given in table 1 for frequencies up to 250 Hz. All uncertainty components are discussed in this section. As mentioned above, the frequency range above 1.5 kHz requires further investigations. A possible reason for the steep increase could be either crosstalk, which increases with rising frequency, or the limited bandwidth / FIR filter of the sampler in combination with resonances in the comparison setup. An unexplained and similarly steep ω^4-increase was found in [28] during the validation of the ac-QVM with thermal converters.

The final sum of the uncertainty contributions for the comparison between the JAWS and the ac-QVM at $1\,V_{RMS}$ and frequencies up to 250 Hz is $11.7\,\mathrm{nV\,V^{-1}}$ ($k = 1$). This uncertainty demonstrates the accuracy of the JAWS—the type-B components for the JAWS alone contribute $5.2\,\mathrm{nV\,V^{-1}}$ ($k = 1$). Furthermore, the type-B contributions solely from the ac-QVM result in an uncertainty of $9.1\,\mathrm{nV\,V^{-1}}$ ($k = 1$). This result is already much smaller than expected from previous investigations of the ac-QVM [28, 29]. The reason is

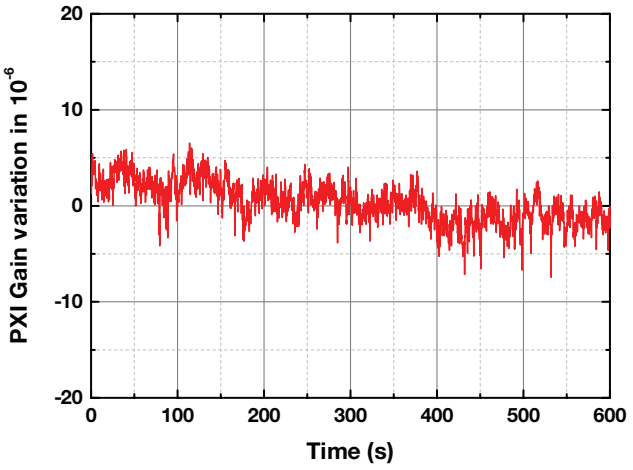

Figure 8. *Gain versus time* trace for the ΣΔ-ADC.

very likely that its uncertainty has been overestimated due to the synthesizers involved in the experimental verifications. An additional reduction of the main contribution, the gain of the ΣΔ-ADC, for low frequencies can be achieved by increasing the number of samples per period used in the ac-QVM. The type-B contributions to the uncertainty budget are discussed in detail in the following paragraphs.

The uncertainty due to the time base is almost negligible as both systems are connected to the same 10 MHz reference. The frequency uncertainty for the compact microwave synthesizer is small and has been evaluated to be of the order of 4×10^{-12} [28]. The 15 GHz clock generator has been evaluated using an EIP frequency counter. A relative frequency difference of only $(-0.6 \pm 1.1) \times 10^{-12}$ has been measured within 10 min.

5.1. ΣΔ-ADC gain

In [28, 29], the error due to variations in the gain, G, of the ΣΔ-ADC could only be estimated as the calibrator noise dominated the uncertainty calculation. Since the JAWS as a quantum standard is stable and has much less noise than a calibrator, we are now able to evaluate this influence. Figure 8 shows the typical variation of G versus time over 10 min. This is the maximum time between the determination of the gain, as explained in section 4.1, and the measurements with the ac-QVM. Gain variations within this time are less than $\pm 5\,\mu\mathrm{V\ V^{-1}}$. We modified the software that reconstructs the waveform at the input of the ac-QVM and deliberately changed the gain by $\pm 30 \times 10^{-6}$. The corresponding changes in the amplitude of the JAWS are presented in figure 9. As expected, the voltage deviations follow the gain variation linearly. The grey region highlights the expected variation in the reconstructed RMS value for the conservative gain changes of $\pm 5\,\mu\mathrm{V\ V^{-1}}$ from figure 8. Assuming a rectangular distribution we achieve an uncertainty $u_G = 15\,\mathrm{nV}/\sqrt{3} = 8.7\,\mathrm{nV}$ ($k = 1$). This value is in agreement with the theoretical estimation in [29].

5.2. ΣΔ-ADC INL

ΣΔ-ADC integral nonlinearities (INL) of up to $4\,\mu\mathrm{V\,V^{-1}}$ have been published [40]. Therefore, we investigated using

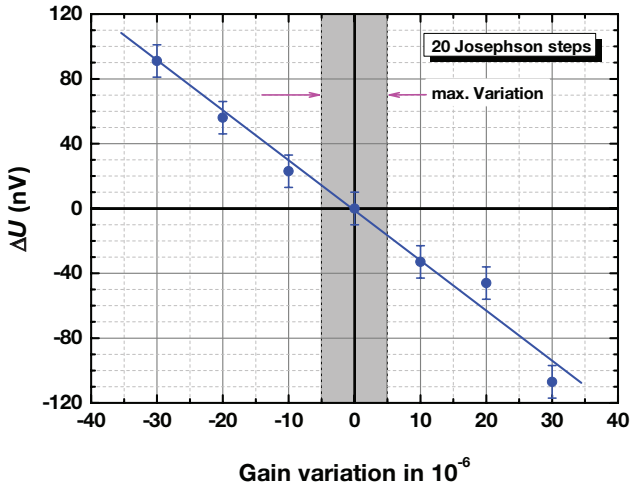

Figure 9. Relative voltage differences in the amplitude of the JAWS for a deliberately changed gain of the ΣΔ-ADC.

a fourth order polynomial to fit the gain of the ΣΔ-ADC. Experimentally we could not find any difference when switching between linear and polynomial approximations of the gain function. The INL of the sampler has little influence on a differentially measured ac voltage, as only a small portion of the complete input range is used in the ac-QVM. Due to the linear gain fit INL contributions cancel out to first order. The resolution of the binary 2 V programmable Josephson array is limited to one step at 70 GHz, ≈ 0.145 mV, which would give an upper limit of $4\,\mu V\ V^{-1} \times 0.145\,mV \times \sqrt{20} = 2.6\,nV$. An uncertainty calculation using a worst case value reported in the literature [40] (based on different gain values for positive and negative voltages) provides as upper limit for INL error in our measurements $u_{INL} = 5\,nV/\sqrt{3} = 2.9\,nV$ ($k = 1$). Further experimental investigations are required for a better estimate of this uncertainty component.

5.3. ΣΔ-ADC bandwidth

The error due to the limited bandwidth of the filter, described in [42], is kept small as we used only 20 Josephson steps per period at a sample rate of at least $4\,MS\,s^{-1}$. There is a change in bandwidth when the sampling frequency is modified. The gain of at least two commercial ΣΔ-ADCs has been observed to depend on the sampling rate used [28, 46]. We only measured a few times at a higher sampling rate of $10\,MS\,s^{-1}$ to verify our results. Whenever we change the sampling rate, we allow the instrument 15 min to reach stable conditions. The change in gain is accounted for in this comparison, as it is measured during the first, JAWS off, step of the sequence of measurements. Based on our measurements (figure 6) and the findings in [21] that no uncertainty contribution for 100 mV voltages at the ΣΔ-ADC for $N \geqslant 16$ and sample rates $\geqslant 4\,MS\,s^{-1}$ needs to be considered we estimate an upper limit for this uncertainty component to $u_{bandwidth} = 5\,nV/\sqrt{3} = 2.9\,nV$ ($k = 1$).

5.4. Cable correction

Due to the differential set-up for the comparison, the input impedance of the ΣΔ-ADC (1 MΩ parallel with 60 pF) presents negligible loading to the Josephson systems. Furthermore, following the discussion from Jeanneret *et al* [21], differences in lead resistance of the JAWS and PJVS can be neglected as well. Only the cable correction for the connection between the JAWS and the sampler has to be taken into account. In our setup, we have a 1.3 m twisted pair cable inside the cryoprobe and a 1 m coaxial cable at room temperature. The correction has quadratic frequency dependence and is of the order of $\omega^2 LC$ with the capacitive and inductive loads of the cables. As described in [21] the correction is small at 500 Hz, and at 250 Hz becomes approximately $0.43\,nV\,V^{-1}$ ($k = 1$). For 1 kHz, the upper bound for correction can be estimated to be $8\,nV\,V^{-1}$. However, cable correction cannot explain the observed increase at higher frequencies (figure 6) as it is too small and opposite in sign.

5.5. On-chip inductance and phase error

An on-chip error due to the array inductance has been evaluated by Landim *et al* [47] and also discussed in [21]. The error voltage appears mainly in quadrature to the Josephson voltage. An in-phase component results from inadequate low frequency filtering by the dc-blocks and by a phase error of the compensation current. This error can be best determined at high frequencies e.g. at 100 kHz. For a single array the error contribution has been estimated to be $25\,nV\,V^{-1}$ for a 10-degrees phase error at 100 mV and 500 Hz [21], which would result in about 35 nV for 1-degree phase error at 250 Hz for 8 arrays.

We have evaluated this contribution at 25 kHz and measured error signals 10 times larger than those published in [47]. We deduce array inductances of 50 nH to 60 nH (array #4 with 9000 junctions), which are also ten times larger than expected. This is probably due to crosstalk making this evaluation method difficult for our cryoprobe with 8 arrays. As we found negligible errors from inadequate low frequency filtering by the dc-blocks and by a compensation current phase error in another cryoprobe with a single array this assumption is supported.

To finally determine this error contribution we made sweeps of the compensation signal phase. In figure 10 the voltage change of array #4 is shown for a phase variation over 14 degrees and for two frequencies, 10 kHz and 25 kHz. The range of operating margins is clearly visible. The central part between ±4 degrees has a slope. Linear fits to the measurement data result in −5.4 nV per degree for 10 kHz and −15 nV per degree for 25 kHz. This means that the slope scales linearly with frequency within the measurement uncertainty. For this array the relative uncertainty becomes $u_{inductance} = 15\,nV / 138\,mV \times 250\,Hz / 25\,kHz = 1.1\,nV\,V^{-1}$. All other arrays have less Josephson junctions and the phase adjustment may result in positive or negative voltages. Therefore, we can estimate an uncertainty contribution $u_{inductance} = 1.1\,nV \times \sqrt{8} = 3.1\,nV$ ($k = 1$) for 8 arrays.

We also have to take into account that we are summing up 8 voltages from 8 arrays. An on-chip phase error when adding up voltages from several arrays causes a reduced voltage $\varepsilon = 1 - \cos(\phi_l + \phi_e)$, as already discussed in [17]. Such a phase error is given by the phase shift due to the cable length

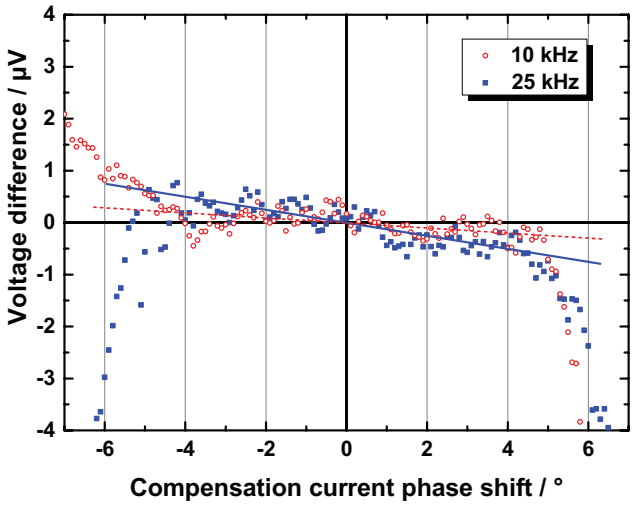

Figure 10. Relative voltage differences in the amplitude of the JAWS (array #4, 138 mV RMS) for compensation current phase trim. The two lines indicate linear fits to slope of the measurements in the range −4° to +4°.

between the arrays, ϕ_l, and the electrical length due to the on-chip filters, ϕ_e. For two arrays on a single chip, the error has been estimated to be 4×10^{-12}V V^{-1} with $\phi_l = (l\ 2\pi f\ c^{-1})$, $l = 10$ cm being the length of the superconducting wire that connects the two arrays, f the frequency and c the speed of light. ϕ_e is the electrical phase shift caused by the on-chip filters 'F' (see figure 2) which can be roughly estimated as phase shift of a parallel *LCR* circuit. Following the estimation of [17], this results in 1.6×10^{-11}V V^{-1} for the combination of 8 arrays on 4 chips as used here.

5.6. Sloped step

Due to the round shape of the quantized plateau of array #8, an unobservable slope cannot be completely excluded. A linear fit of the central part of the step in figure 4 between −30 µA and +40 µA yields a slope of 0.72 nV µA^{-1}. The resolution and stability of our bias current over the duration of the measurements, as described above, is better than 1 µA. As explained above, for each frequency an adjustment of the compensation amplitude is made similarly to a few readjustments at 250 Hz. Due to different settings below and above the step centre a systematic error is almost cancelled. As an upper uncertainty limit we can use a conservative value of 10 µA, thus producing an $u_{\mathrm{Slope}} = 10\,\mu\mathrm{A} \times 0.72\,\mathrm{nV}\,\mu\mathrm{A}^{-1}/\sqrt{3} = 4.2\,\mathrm{nV}$ ($k = 1$).

6. Conclusion

The newly developed 1 V RMS Josephson arbitrary waveform synthesizer (JAWS) at PTB [4] has been further improved. Crosstalk has been reduced and higher harmonics are now suppressed at least by 121 dBc. Its accuracy is evaluated by performing a direct comparison with an ac quantum voltmeter. The result for the direct comparison at 250 Hz shows excellent agreement between the two quantum standards $V_{\mathrm{JAWS}} - V_{\mathrm{ac\text{-}QVM}} = +3.5$ nV with a type-A standard deviation of the mean of 5.0 nV ($k = 1$) ($+3.5 \pm 5.0 \times 10^{-9}$ in relative units). Uncertainty components have been evaluated in detail. The combined overall uncertainty for the direct comparison is 11.7 nV, and the final result of the comparison $V_{\mathrm{JAWS}} - V_{\mathrm{ac–QVM}} = (+3.5 \pm 11.7) \times 10^{-9}$ in relative units ($k = 1$). This result is an improvement from previous comparisons by one order of magnitude [21] and also better as in a previous on-chip comparison at a lower voltage level [17]. We have further demonstrated that the quantum accuracy of the 1 V RMS JAWS is about one order of magnitude better than conventional ac–dc transfer standards [13, 14]. In addition, the comparison establishes the potential of the ac-QVM for measuring ac voltages with an uncertainty of 10^{-8} ($k = 1$) for frequencies up to 500 Hz. This comparison has removed the former limitation due to the waveform generator (calibrator) being measured by the ac-QVM [28, 29].

Finally, the frequency dependence above 1 kHz needs further investigations to understand the limitations of both systems at higher frequencies. For future work, a direct Josephson comparison with a second pulse-driven ac Josephson voltage standard can be made to determine the real limit of the JAWS.

Acknowledgment

The authors would like to acknowledge Helko van den Brom, Ernest Houtzager (both VSL), Alexander Katkov (VNIIM), Marco Schubert (Supracon and PTB), Franz Ahlers and Thomas Hagen (both PTB) for fruitful discussions. We also thank Rüdiger Wendisch, Peter Duda, Gerd Muchow, Helena Derr and Michael Busse (all PTB) for technical support.

This work was partly carried out with funding by the European Union within the EMRP JRPs AIM QuTE and Q-WAVE. The EMRP is jointly funded by the EMRP participating countries within EURAMET and the European Union.

References

[1] Benz S P and Hamilton C A 1996 A pulse-driven programmable Josephson voltage standard *Appl. Phys. Lett.* **68** 3171–3

[2] Benz S P, Waltman S B, Fox A E, Dresselhaus P D, Rüfenacht A, Underwood J M, Howe L, Schwall R E and Burroughs C J 2015 1 V Josephson arbitrary waveform synthesizer *IEEE Trans. Appl. Supercond.* **25** 1300108

[3] Benz S P, Waltman S B, Fox A E, Dresselhaus P D, Rüfenacht A, Howe L, Schwall R E and Flowers-Jacobs N E 2015 Performance improvements for the NIST 1 V Josephson arbitrary waveform synthesizer *IEEE Trans. Appl. Supercond.* **25** 1400105

[4] Kieler O F, Behr R, Wendisch R, Bauer S, Palafox L and Kohlmann J 2015 Towards a 1 V Josephson arbitrary waveform synthesizer *IEEE Trans. Appl. Supercond.* **25** 1400305

[5] Benz S P, Burroughs C J Jr, Dresselhaus P D, Bergren N F, Lipe T E, Kinard J R and Tang Y 2007 An ac Josephson voltage standard for ac–dc transfer standard measurements *IEEE Trans. Instrum. Meas.* **56** 239–43

[6] Lipe T E, Kinard J R, Tang Y-H, Benz S P, Burroughs C J and Dresselhaus P D 2008 Thermal voltage converter

calibrations using a quantum ac standard *Metrologia* **45** 275–80
[7] Houtzager E, Benz S P and van den Brom H E 2009 Operating margins for a pulse-driven Josephson arbitrary waveform synthesizer using a ternary bit-stream generator *IEEE Trans. Instrum. Meas.* **58** 775–80
[8] Filipski P S, van den Brom H E and Houtzager E 2012 International comparison of quantum ac voltage standards for frequencies up to 100 kHz *Measurement* **45** 2218–25
[9] Kieler O F O, Landim R P, Benz S P Dresselhaus P D and Burroughs C J 2008 ac–dc transfer standard measurement and generalized compensation with the ac Josephson voltage standard *IEEE Trans. Instrum. Meas.* **57** 791–6
[10] Toonen R C and Benz S P 2009 Nonlinear behavior of electronic components characterized with precision multitones from a Josephson arbitrary synthesizer *IEEE Trans. Appl. Supercond.* **19** 715–8
[11] Schleussner D, Kieler O F, Behr R, Kohlmann J and Funck T 2010 Investigations using an improved Josephson arbitrary waveform synthesizer (JAWS) system *Conf. Dig. CPEM 2010* (*Daejeon, Korea, 2010*) pp 177–8
[12] Hagen T, Budovsky I, Benz S P and Burroughs C J 2012 Calibration system for ac measurement standards using a pulse-driven Josephson voltage standard and an inductive divider *Conf. Dig. CPEM 2012* (*Natl. Harbor, USA, 2012*) pp 672–3
[13] Klonz M 2002 CCEM-K6.a: key comparison of ac–dc transfer standards at the lowest attainable level of uncertainty *Metrologia Tech. Suppl.* **39** 01002–1
[14] Budovsky I *et al* 2005 APMP international comparison of ac–dc transfer standards at the lowest level of attainable uncertainty *IEEE Trans. Instrum. Meas.* **54** 795–8
[15] Behr R, Kieler O F O, Schleussner D, Palafox L and Ahlers F 2013 Combining Josephson systems for spectrally pure ac waveforms with large amplitudes *IEEE Trans. Instrum. Meas.* **62** 1634–9
[16] Behr R, Kieler O, Kohlmann J, Müller F and Palafox L 2012 Development and metrological applications of Josephson arrays at PTB *Meas. Sci. Technol.* **23** 124002
[17] Kieler O F, Behr R, Schleussner D, Palafox L and Kohlmann J 2013 Precision comparison of sine waveforms with pulse-driven Josephson arrays *IEEE Trans. Appl. Supercond.* **23** 1301404
[18] Benz S P, Dresselhaus P D, Burroughs C J and Bergren N F 2007 Precision measurements using a 300 mV Josephson arbitrary waveform synthesizer *IEEE Trans. Appl. Supercond.* **17** 864–9
[19] Benz S P, Burroughs C J and Dresselhaus P D 2001 AC coupling technique for Josephson waveform synthesis *IEEE Trans. Appl. Supercond.* **11** 612–6
[20] Kohlmann J, Kieler O F, Iuzzolino R, Lee J, Behr R, Egeling B and Mueller F 2009 Development and investigation of SNS Josephson arrays for the Josephson arbitrary waveform synthesizer *IEEE Trans. Instrum. Meas.* **58** 797–802
[21] Jeanneret B, Rüfenacht A, Overney F, van den Brom H E and Houtzager E 2011 High precision comparison between a programmable and a pulse-driven Josephson voltage standard *Metrologia* **48** 311–6
[22] Lipe T L and Kinard J R 2012 Quantum ac voltage standards 2012 *IEEE Trans. Instrum. Meas.* **61** 2160–6
[23] Behr R, Palafox L, Ramm G, Moser H and Melcher J 2007 Direct comparison of Josephson waveforms using an ac quantum voltmeter *IEEE Trans. Instrum. Meas.* **56** 235–8
[24] Rufenacht A, Burroughs C J, Benz S P, Dresselhaus P D, Waltrip B C and Nelson T L 2009 Precision differential sampling measurements of low-frequency synthesized sine waves with an ac programmable Josephson voltage standard *IEEE Trans. Instrum. Meas.* **58** 809–15
[25] Kim M-S, Kim K-T, Kim W-S, Chong Y and Kwon S-W 2010 Analog-to-digital conversion for low-frequency waveforms based on the Josephson voltage standard *Meas. Sci. Technol.* **21** 115102
[26] Williams J M, Henderson D, Pickering J, Behr R, Müller F and Scheibenreiter P 2011 Quantum-referenced voltage waveform synthesiser *Sci. Meas. Technol. IET* **5** 167–74
[27] Rüfenacht A, Burroughs C J, Dresselhaus P D and Benz S P 2013 Differential sampling measurement of a 7 V RMS sine wave with a programmable Josephson voltage standard *IEEE Trans. Instrum. Meas.* **62** 1587–93
[28] Lee J, Behr R, Palafox L, Schubert M, Starkloff M and Böck A C 2013 An ac quantum voltmeter based on a 10 V programmable Josephson array *Metrologia* **50** 612–22
[29] Schubert M, Starkloff M, Lee J, Behr R, Palafox L, Boeck A C, Fleischmann P and May T 2015 An ac Josephson voltage standard up to the kHz range tested in a calibration laboratory *IEEE Trans. Instrum. Meas.* at press
[30] Behr R, Palafox L and Kohlmann J 2008 Improvements of the ac quantum voltmeter *Conf. Dig. CPEM 2008* (*Broomfield, USA, 2008*) pp 44–5
[31] Behr R, Henderson D, Williams J M, Palafox L, Lee J and Pickering J 2010 Operation of the ac quantum voltmeter at kHz frequency *Conf. Dig. CPEM 2010* (*Daejeon, Korea, 2010*) pp 93–4
[32] Kleinschmidt P, Patel P D, Williams J M and Janssen T J B M 2002 Investigation of binary Josephson arrays for arbitrary waveform synthesis *IEE Proc. Sci. Meas. Technol.* **149** 313–6
Patel P D, Williams J M and Janssen T J B M 2001 A programmable bias source for binary Josephson junction arrays *Proc. BEMC* (*Harrogate, UK*)
[33] Muller F, Scheller T, Wendisch R, Behr R, Kieler O, Palafox L and Kohlmann J 2013 NbSi barrier junctions tuned for metrological applications up to 70 GHz: 20 V arrays for programmable Josephson voltage standards *IEEE Trans. Appl. Supercond.* **23** 1101005
[34] Robinson I A 1991 An optical-fiber ring interface bus for precise electrical measurements *Meas. Sci. Technol.* **2** 949–56
[35] Williams J M, Henderson D, Patel P, Behr R and Palafox L 2007 Achieving sub- 100 ns switching of programmable Josephson arrays *IEEE Trans. Instrum. Meas.* **56** 651–4
[36] Jülicher Squid GmbH (www.jsquid.com)
[37] Watanabe M, Dresselhaus P D and Benz S P 2006 Resonance-free low-pass filters for the ac Josephson voltage standard *IEEE Trans. Appl. Supercond.* **16** 49–53
[38] Lee J, Behr R, Palafox L, Schubert M, Starkloff M and Böck A C 2012 A voltage calibrator based on programmable Josephson arrays *Conf. Dig. CPEM 2012* (*Natl. Habor, USA, 2012*) pp 40–1
[39] Lee J, Nissilä J, Katkov A and Behr R 2014 A quantum voltmeter for precision measurements *Conf. Dig. CPEM 2014* (*Rio de Janeiro, Brazil, 2014*) pp 732–3
[40] Overney F, Rufenacht A, Braun J, Jeanneret B and Wright P S 2011 Characterization of metrological grade analog-to-digital converters using a programmable Josephson voltage standard *IEEE Trans. Instrum. Meas.* **60** 2172–7
[41] NI PXI/PCI-5922 Specification (www.ni.com/pdf/manuals/374049e.pdf)
[42] Rüfenacht A, Overney F, Mortara A and Jeanneret B 2011 Thermal-transfer standard validation of the Josephson-voltage-standard-locked sine-wave synthesizer *IEEE Trans. Instrum. Meas.* **60** 2372–7
[43] Jeanneret B, Overney F, Callegaro L, Mortara A and Rüfenacht A 2009 Josephson-voltage-standard-locked sine

wave synthesizer: margin evaluation and stability *IEEE Trans. Instrum. Meas.* **58** 791–6
[44] Witt T J 2007 Using the autocorrelation function to characterize time series of voltage measurements *Metrologia* **44** 201–9
[45] van den Brom H E and Houtzager E 2012 Expanding the operating range of the pulse-driven ac Josephson voltage standard *Conf. Dig. CPEM 2012* (*National Harbor, USA 2012*) pp 42–3
[46] Rietveld G, Zhao D, Kramer C, Houtzager E, Kristensen O, de Leffe C and Lippert T 2011 Characterization of a wideband digitizer for power measurements up to 1 MHz *IEEE Trans. Instrum. Meas.* **60** 2195–201
[47] Landim R P, Benz S P, Dresselhaus P D and Burroughs C J 2008 Systematic-error signals in the ac Josephson voltage standard: measurement and reduction *IEEE Trans. Instrum. Meas.* **57** 1215–20